Application of Mathematical Absorber Reflection Suppression to Far-Field Antenna Measurements

S.F. Gregson[#1], J. Dupuy[*2], C.G. Parini[*3], A.C. Newell[#4], G.E. Hindman[#5]

[#]*Nearfield Systems Inc.*
19730 Magellan Drive, Torrance, CA 90502, USA
[1]sgregson@nearfield.com
[4]anewell@nearfield.com
[5]ghindman@nearfield.com

[*]*Queen Mary, University of London*
Mile End Road, London E1 4NS, UK
[2]john.dupuy@eecs.qmul.ac.uk
[3]c.g.parini@eecs.qmul.ac.uk

***Abstract*— For some time now, a technique named Mathematical Absorber Reflection Suppression (MARS) has been used successfully to identify and then suppress range multi-path effects in spherical [1, 2, 3, 4], cylindrical [5, 6, 7], and planar [8, 9] near-field antenna measurement systems. This paper details a recent advance that, for the first time, allows the MARS measurement and post-processing technique to be successfully deployed to correct antenna pattern data taken using direct far-field or compact antenna test ranges (CATRs) where only a single great circle cut is acquired. This paper provides an overview of the measurement and novel data transformation and post-processing chain that is utilised within the far-field MARS (F-MARS) technique to efficiently correct far-field, frequency domain data. Preliminary results of range measurements that illustrate the success of the technique are presented and discussed.**

I. Introduction

The far-field antenna radiation pattern is characterised by exhibiting a spatial variation that has a purely angular dependence, *i.e.* an: angular amplitude variation, angular phase variation and angular polarisation variation. Ideally, all of these properties can be determined by placing a test antenna in a perfectly uniform, homogeneous, plane wave field and mechanically rotating it about the relevant angular co-ordinate system whilst measuring the received amplitude and/or phase. In practice, perhaps the most basic direct method is to generate the plane wave from a small portion of a spherical wave-front. This can be achieved by placing a low gain source antenna at a large distance from the antenna under test (AUT) so that the field incident across the AUT's aperture closely approximates a plane-wave. Although there are a great many ways in which the plane wave illumination of the AUT can be achieved in practice, their mechanisms can be considered to divide into two categories, direct and indirect collimation. Those that rely upon direct collimation include free-space ranges, reflection ranges, that is compact antenna test ranges (CATRs) and refraction, that is dielectric lens ranges. Conversely, indirect techniques include all forms of near-field ranges. The popularity of direct collimating antenna range measurements can perhaps be seen to stem from the simplicity with which far-field parameters can be obtained from the experimental equipment, the absence of a requirement to undertake intensive mathematical analysis before useful results are obtained, and the ability to acquire zero-dimensional (*e.g.* boresight) and one-dimensional (*e.g.* great circle cut) pattern data.

Reflections in antenna test ranges can often be the largest source of measurement error within the error budget of a given facility [10] with direct collimating ranges being perhaps the most susceptible to these contaminants [11]. Considerable attention has been paid to range multipath suppression in the open literature with significant effort, ingenuity and resourcefulness having been devoted to quantifying and subsequently compensating multi-path contaminated measurements by means of: hardware or software time-gating, background subtraction, or complex plane circular least squares fitting. Until now, the mode orthogonalisation and filtering techniques that have proved so overwhelmingly successful in near-field ranges (planar, cylindrical, spherical) have not previously been applied to two-dimensional far-field measurements. Thus for the first time, this paper describes a measurement and mathematical post processing technique that requires only a minimum amount of information about the AUT and measurement geometry, and which suppresses reflections in a direct far-field one-dimensional antenna range measurement. The processing is applied efficiently to the interferometric frequency domain far-field data through the use of the fast Fourier transform (FFT) algorithm. This technique is entirely generic in nature, and can be applied to a variety of different antenna types with no specific a priori assumptions being made about the distribution of the currents over the AUT.

II. Overview Of The Far-Field MARS Technique

It is well known that the far-fields of an antenna can be represented as a linear superposition of orthogonal cylindrical mode coefficients. However, it has only recently been shown that this permits the application of cylindrical mode orthogonalisation and filtering algorithms to suppress

reflections within measurements made using non cylindrical systems [8, 9]. This observation permits the MARS technique to be applied to many different measurement systems, including direct collimating ranges. Contrary to usual antenna measurement practice, the MARS technique deliberately displaces the AUT from the centre of rotation. This has the effect of making the differences in the illuminating field far more pronounced than would otherwise be the case, and it is exactly this greater differentiation that makes their identification and subsequent extraction viable. Figure 1 below shows an AUT installed within a typical spherical geometry measurement system, centred about the origin of the range co-ordinate system, and the conceptual smallest sphere that circumscribes the majority of the current sources which is centred on the intersection of the rotational axes (shown as red lines). Conversely, Figure 2 shows an equivalent MARS measurement where the AUT has been displaced away from the centre of rotation and the maximum radial extent (MRE) has been correspondingly increased.

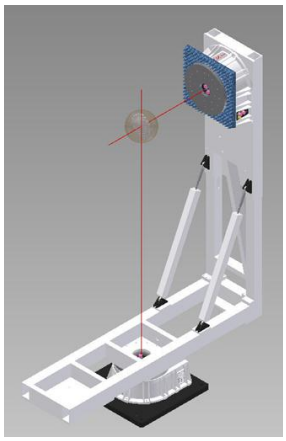

Fig. 1 AUT measured conventionally at rotation origin with smaller MRE shown.

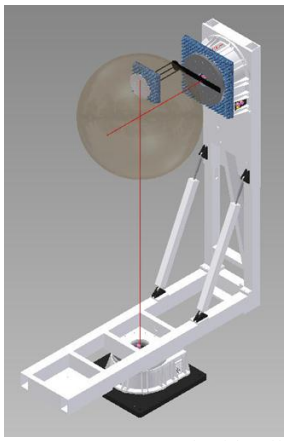

Fig. 2 AUT measured with offset from rotation origin with larger MRE shown.

Once the far-field great circle pattern cut has been acquired and the AUT has been mathematically translated back to the origin of the measurement co-ordinate system by means of a differential phase change [12], the equivalent cylindrical mode coefficients (CMCs) can be deduced from far electric fields using standard cylindrical near-field theory [5, 6, 7],

$$B_n^1(\gamma) = -\frac{(-j)^{-n}}{4\pi\kappa}\int_0^{2\pi} E_\phi(r\to\infty,\theta,\phi)e^{-jn\phi}d\phi \qquad (1)$$

$$B_n^2(\gamma) = -j\frac{(-j)^{-n}}{4\pi\kappa}\int_0^{2\pi} E_\theta(r\to\infty,\theta,\phi)e^{-jn\phi}d\phi \qquad (2)$$

Here, ϕ represents a rotation about the vertical axis while θ is measured away from the positive vertical axis. The additional factor of 2π is introduced in the denominator of equations (1) and (2) to enforce the correct normalisation of the CMCs, *c.f.* equations (4) and (5). From examination of equations (1) and (2), it is clear that for a fixed value of θ it is possible to deduce all CMCs for a corresponding value of γ. It is this observation that allows the MARS technique to be extended and applied to two-dimensional far-field applications as when processing great circle far-field cuts, the polar angle $\theta = \pi/2$. Once the cylindrical mode coefficients for the, now ideally centrally located, AUT have been recovered, any mode representing fields outside the ideal conceptual minimum MRE can be filtered out thereby removing contributions that are not associated with the AUT. Thus, from standard cylindrical theory [5, 6, 7], it is possible to filter out all higher order modes without affecting the integrity of the underlying antenna pattern function. When expressed mathematically the band-pass brick-wall mode filter function can be expressed as,

$$B_n^s(\gamma)\big|_{s=1,2} = \begin{cases} B_n^s(\gamma) & n^2 + (\gamma r_{t0})^2 \le (k_0 r_{t0})^2 \\ 0 & \text{elsewhere} \end{cases} \qquad (3)$$

It is clear that the CMCs associated with the AUT are confined to a narrow band that are tightly distributed about the $n = 0$ CMC. As the total power radiated by the AUT must be conserved, the amount of power per mode must increase as the total number of modes associated with the AUT decreases. As the amount of noise per mode can be seen to be roughly constant with respect to the maximum level, the effective system signal to noise (SNR) ratio of the measurement is significantly increased. Crucially, and as has been observed previously with all other MARS implementations, although the AUT has been translated back to the origin of the measurement co-ordinate system, this is not the case for the scatterers which are spatially extended and are represented by many *higher* order modes. In effect, the contributions in the CMC domain of the AUT and the scatterers are separated so that they do not interfere and are in essence orthogonalised from one another. The asymptotic MARS processed far-field pattern can be obtained from a simple summation of CMCs as follows [5, 6, 7],

$$E_\theta(r\to\infty,\theta,\phi) = 2jk_0\sin\theta\sum_{n=-\infty}^{\infty}(-j)^n B_n^2(\gamma)e^{jn\phi} \qquad (4)$$

$$E_\phi(r\to\infty,\theta,\phi) = -2k_0\sin\theta\sum_{n=-\infty}^{\infty}(-j)^n B_n^1(\gamma)e^{jn\phi} \qquad (5)$$

$$E_r(r\to\infty,\theta,\phi) = 0 \qquad (6)$$

Here, and as per the usual convention, the unimportant far-field spherical phase factor and inverse r term have been suppressed. As these transforms and their inverse operations can be evaluated with the fast Fourier transform (FFT) this makes the F-MARS algorithm very efficient in terms of computational effort.

III. Experimental Verification

The Queen Mary, University of London (QMUL) mm-wave Compact Antenna Test Range (CATR) comprises a single offset reflector antenna of 3 metres in diameter and is constructed from 18 individual high precision panels. These panels were developed and manufactured at the Rutherford Appleton Laboratories, UK, for the James Clerk Maxwell Telescope. The individual panels have a measured average root mean squared (RMS) surface accuracy of between 8 and 15 microns. Each panel has three, micrometer adjustable, mounting points and are individually aligned using a two theodolite method giving an overall surface RMS accuracy of approximately 90 microns. An anechoic chamber completely encloses the mm-wave CATR which has been used for

measurements in the frequency range 5 to 200 GHz with a quiet zone size, defined by ripple of ±0.5 dB and ±5°, of approximately 1 metre in diameter. The turntable system is mounted on linear rails providing down range movement and has a hydraulic platform to provide height adjustment along with a precision cross slide providing transverse horizontal movement. Turntable control is via an Orbit AL 4806-3C controller which is linked to QMUL in-house measurement software. The QMUL CATR is described in detail in [13]. Data acquired using the QMUL CATR was tabulated as a function of angle. However, the measurements were taken at regular time steps since this process was known to be the most accurate technique for recording data within this facility. Although the data was sampled on an irregular, grid that was not necessarily monotonic, it was grossly over sampled with typically 15 samples being taken per degree. This irregularly spaced data was subsequently re-tabulated using cubic spline interpolation onto a convenient, equally spaced, monotonic grid in order that the necessary post processing could be performed efficiently. Polar (*i.e.* amplitude and phase) interpolation was utilised whereby the re-tabulation process was performed separately on the square root of the magnitude of the field, and modulo 2π phase function. The phase data was initially unwrapped by changing all absolute jumps of greater than π to their 2π complement, in order that any $\pm\pi$ phase discontinuities would not destabilise the interpolation process. All data obtained from this facility was processed using this regularisation method.

In order that an estimate of the upper bound error that this approximation inevitably introduces could be obtained, the regularised data was interpolated back onto the measurement grid using sampling functions [12]. This interpolation scheme is rigorous, *i.e.* exact, as the acquired data is spectrally band-limited. This technique relies upon the data being tabulated on a uniformly spaced grid thus; it cannot be used in place of the approximate polynomial method described above. Figure 3 below contains a representative plot showing the measured data where a corrugated horn was used as an AUT overlaid with the reconstructed measured data that was formed from the regularised data set. Plotted with these traces is the 21 point boxcar mean average of the equivalent multipath level (EMPL) that can be taken to constitute an upper bound uncertainty level for this data regularisation process [12].

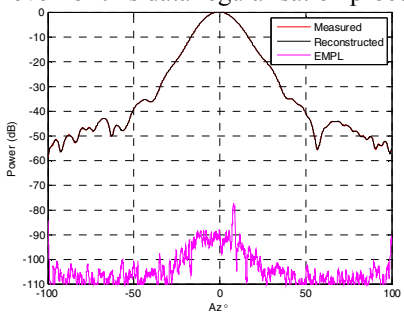

Fig. 3 Upper bound uncertainty of data regularisation process.

Clearly, the EMPL trace is more than 75 dB below the boresight values and *circa* 60 dB lower in the region of the wide-out sidelobes. Providing all EMPL traces are found to be above this level when comparing between reference and MARS corrected patterns, any small errors introduced by this regularisation processing can be effectively ignored.

In the absence of some overriding definitive standard or infallible model, the only practical methodology for assessing the effectiveness of a measurement system is by way of measurement repetition. This repetition can be accomplished without alteration of the measurement configuration, to simply address repeatability, or with the inclusion of parametric variations it can be used to assess sensitivity. In this case, repeat measurements were taken of the far-field great circle azimuth cut of a medium gain (aperture diameter 127mm) x-band corrugated horn where a single parametric change was introduced into the measurement. This change consisted of introducing a 0.6 m by 0.6 m flat reflecting plate into the chamber that was located in the same horizontal plane as the AUT and was chosen as it constituted a worst case configuration as the specular reflection of the main beam of the corrugated horn directly illuminated the CATR reflector. This arrangement can be seen presented in Figure 4 below where the AUT was displaced backward from the centre of rotation by 195.1 mm.

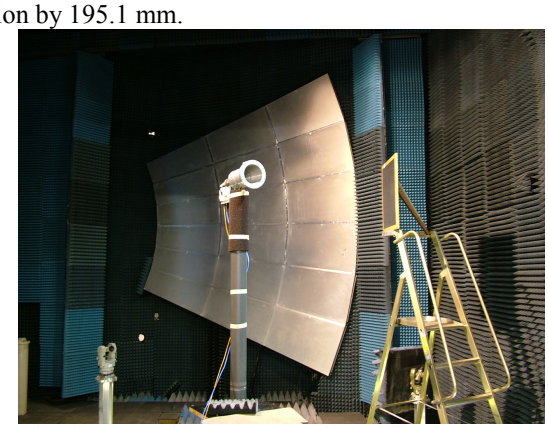

Fig. 4 X-band corrugated horn AUT installed within QMUL CATR shown together with 0.6 m by 0.6 m reflecting plate, shown to right of picture.

Figure 5 and 6 below contain, respectively, plots of the great-circle far-field co-polar amplitude and phase patterns of the AUT where the blue (reference) traces were taken without the reflecting plate. Conversely, the red traces were taken with the reflecting plate installed within the chamber and they clearly show the effects of the additional scattering as an additional large amplitude side-lobe at around $Az = 50°$.

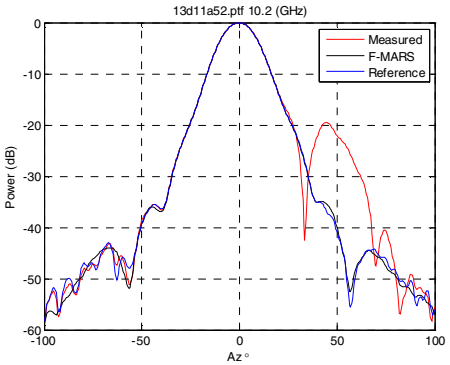

Fig. 5 Far-field plot of x-band corrugated horn power pattern measured with and without reflecting plate plotted against F-MARS processed pattern.

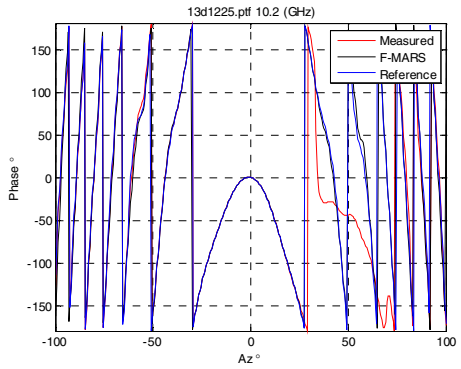

Fig. 6 Far-field plot of x-band corrugated horn phase pattern measured with and without reflecting plate plotted against F-MARS processed pattern.

The measured far-field great circle cut with scattering contamination was post-processed using the F-MARS mode orthogonalisation and filtering algorithm, described above, was used to recover the black traces that can also be seen plotted in Figures 5 and 6. From inspection of these plots, it can be seen that the effects of the spurious scatterer have been effectively suppressed in both the amplitude and phase plots as the respective traces are clearly in very encouraging agreement. Corrugated horns are generally renowned for their excellent symmetry. It is clear that the F-MARS processed patterns demonstrated a very high deal of symmetry as $f(Az)$ is approximately equal to $f(-Az)$ where f denotes the amplitude or phase function. This is a further measure of the success of the technique.

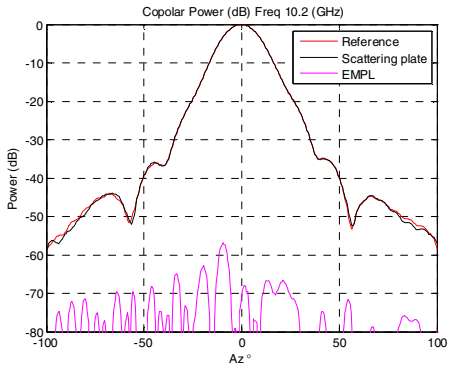

Fig. 7 Comparison of F-MARS processed AUT patterns with and without flat reflecting plate installed within the test environment.

Figure 7 above contains a plot of the F-MARS processed far-field great circle cuts of the corrugated horn that were taken with, and without, the 0.6 m by 0.6 m flat reflecting plate together with the EMPL that is used to quantitatively represent the similarity between the respective measurements. From inspection of Figure 7 it is clear that the patterns are in encouraging agreement and this is further demonstrated by the EMPL which is below -70 dB in the region where the specular reflection had greatest impact. Interestingly, the wide angle high angular frequency ripple that is known to result from diffraction from the edges of the main offset reflector of the CATR have also been suppressed by the F-MARS processing, *c.f.* pattern ripple for $|Az| > 60°$ [12]. However, this effect will clearly require further investigation and verification before more general conclusions can be drawn. Although the results presented above show pattern data limited to the range $|Az| \leq 100°$, which is merely a sector of a great circle, the F-MARS technique itself is capable of processing pattern data over a complete ±180° angular range.

IV. Summary And Conclusions

Far-field MARS processing can be used with a very high degree of confidence since all the steps in the measurement and analysis are consistent with the well-established principles of standard cylindrical near-field theory and measurement technique, and all comparisons thus far have proved overwhelmingly positive. The offset of the AUT and the resulting finer sample spacing are estimated using conventional rules, and the mathematical translation of the AUT to the origin is rigorous. The selection of the mode cut-off for the translated pattern is based on the physical dimensions of the AUT and its translated location. The final result with MARS processing can be degraded if the translation of the AUT is incorrectly applied, or the mode filter is too tight, *i.e.* abrupt, but importantly these parameters are controlled by the user. The results of far-field MARS processing will reduce but cannot entirely eliminate the effect of scattering. As has been demonstrated, this novel frequency domain measurement and processing technique is entirely general and can be used to achieve acceptable results with use of minimal absorber or without the use of an anechoic chamber, even when testing lower gain antennas. MARS has been found to improve the reflection levels in traditional anechoic chambers allowing improved accuracy as well as offering the ability to use existing chambers down to lower frequencies than the absorber might otherwise suggest.

References

[1] G.E. Hindman, A.C. Newell, "Spherical Near-Field Self-Comparison Measurements", AMTA 26th Annual Meeting & Symposium, Atlanta, GA, October 2004.

[2] G.E. Hindman, A.C. Newell, "Reflection Suppression in a large spherical near-field range", AMTA 27th Annual Meeting & Symposium, Newport, RI, October. 2005.

[3] G.E. Hindman, A.C. Newell, "Reflection Suppression To Improve Anechoic Chamber Performance", AMTA Europe 2006, Munich, Germany, March 2006.

[4] G.E. Hindman, A.C. Newell, "Mission To MARS – In Search of Antenna Pattern Craters", AMTA 28th Annual Meeting & Symposium, St. Louis, MO, November 2007.

[5] S.F. Gregson, A.C. Newell, G.E. Hindman, "Reflection Suppression In Cylindrical Near-Field Antenna Measurement Systems – Cylindrical MARS", AMTA 31st Annual Meeting & Symposium, Salt Lake City, UT, November 2009.

[6] S.F. Gregson, A.C. Newell, G.E. Hindman, "Reflection Suppression In Cylindrical Near-Field Measurements of Electrically Small Antennas", Loughborough Antennas & Propagation Conference, November, 2009.

[7] S.F. Gregson, A.C. Newell, G.E. Hindman, M.J. Carey, "Advances in Cylindrical Mathematical Absorber Reflection Suppression", 4th European Conference on Antennas and Propagation, Barcelona, 12th -16th April, 2010.

[8] S.F. Gregson, A.C. Newell, G.E. Hindman, M.J. Carey, "Extension of The Mathematical Absorber Reflection Suppression Technique To The Planar Near-Field Geometry", AMTA, Atlanta, October 2010

[9] S.F. Gregson, A.C. Newell, G.E. Hindman, M.J. Carey, "Application of Mathematical Absorber Reflection Suppression to Planar Near-field Antenna Measurements", 5th European Conference on Antennas and Propagation, Rome, 11th – 15th April, 2011.

[10] A.C. Newell, "Error Analysis Techniques for Planar Near-field Measurements", IEEE Transactions on Antennas and Propagation, vol. AP-36, pp. 754-768, June 1988.

[11] G.E. Evans, "Antenna Measurement Techniques", Artech House, 1990.

[12] S.F. Gregson, J. McCormick, C.G. Parini, "Principles of Planar Near-Field Antenna Measurements", The Institution of Engineering and Technology, UK, 2007.

[13] A.D. Olver, C.G. Parini, "Milimeterwave Compact Antenna Test Ranges", JINA November 1992, Nice.